

Mechanical Design of the Pinhole Imaging System in the APS Storage Ring

S. Sharma, B.X. Yang, A. Barcikowski, B. Rusthoven, and E. Rotela
Advanced Photon Source, Argonne National Laboratory, Argonne, Illinois, USA

Abstract

The new low-emittance lattice of the APS storage ring has reduced the vertical electron beam size to 10-15 μm . A new pinhole imaging system was installed recently in one of the storage ring sectors to image this smaller beam size with sufficient stability and resolution. An upstream absorber is used in this imaging system to limit the incident power on the water-cooled, four-scraper pinhole. Each of the four scrapers is attached to its own translation stage in order to control the size and location of the pinhole. The translation stages are mounted on a support frame designed to reduce vibrational and thermal effects. The mechanical design of the imaging system is presented in this paper.

1. Introduction

The Advanced Photon Source (APS) is a third-generation synchrotron radiation facility based on a 7-GeV electron storage ring. The high brightness of the x-ray beam generated by over twenty undulators distributed around the ring is closely related to the low emittance of the electron beam. Hence the emittance of the electron beam is not only one of the crucial electron beam parameters to be monitored and archived continuously during user operations, it is also one to be optimized during machine physics studies.

Since the vertical dimension of the electron beam is well below the diffraction limit of visible light imaging, the APS adopted x-ray imaging as the main approach for gathering emittance measurements in the early days of its operation. An x-ray pinhole system installed in the Diagnostics Sector 35 was chosen as the workhorse for the day-to-day operation due to its simplicity [1]. Over the years, we learned to deal with artifacts caused by vibrations of the components, power loading, temperature variations, radiofrequency electronic interference, etc. The signal-to-noise ratio improved so much over this period that the pinhole camera data could demonstrate the minute changes in beam size due to users opening and closing the undulator gap [2].

The pinhole currently in use has water-cooled tungsten slits located 9 m from the bending magnet source 35-BM, a YAG scintillation crystal converter located 7.6 m from the pinhole slits, and a lead-shielded CCD camera for reading out the image. The rms resolution of pinhole camera system was measured to be 22 μm using skew-quad scans at very low vertical couplings [2]. This resolution can be compared to the original design beam size of 110 μm for a beam with a total emittance of 9 nm-rad and 10% vertical coupling. In the past seven years of operation, however, the emittance of the storage ring has decreased by a factor three to 3 nm-rad [3], and the vertical beam size has been reduced to the 10-15 μm range during machine studies. This has necessitated an upgrade of the existing pinhole imaging system in order to improve its resolution.

2. Resolution of a Pinhole Imaging System

The resolution of a pinhole imaging system can be best modelled with Fresnel diffraction [4]. Its conclusion can be summarized as in Figure 1. The rms resolution of the pinhole camera is a function of pinhole aperture, d_p , and the wavelength of the x-ray, λ . The optimal resolution, $\sigma_s^{(\min)} \approx a_s/3$, is obtained when the aperture width is set at $d_p^{(\min)} \approx 1.4a_p$, where a_p and a_s are defined as

$$a_p(\text{Natural Unit @ Pinhole}) = \sqrt{\lambda f},$$

and

$$a_s(\text{Natural Unit @ Source}) = \sqrt{\lambda f} \left(1 + \frac{1}{M} \right) = \sqrt{\lambda S \left(1 + \frac{1}{M} \right)},$$

with f and M given by

$$\frac{1}{f} = \frac{1}{S} + \frac{1}{S'} \quad \text{and} \quad M = \frac{S'}{S},$$

where S and S' are the source and detector distances from the pinhole aperture, respectively.

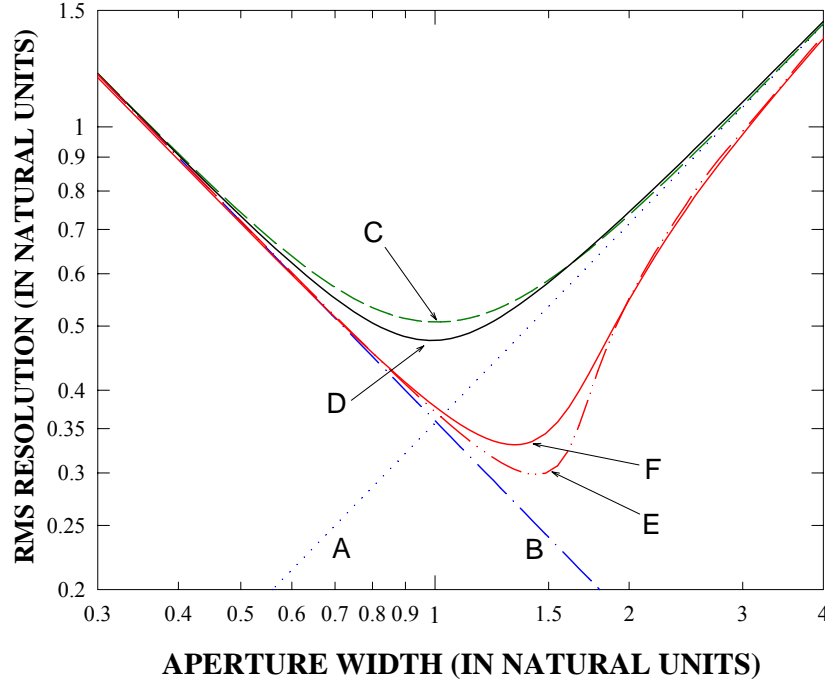


Figure 1: Effective width of the point spread functions from (A) geometrical projection, (B) Fraunhofer diffraction, (C) naïve hybrid model, (D) true hybrid model, (E) monochromatic Fresnel model, and (F) polychromatic Fresnel model with the RMS energy spread 30%.

For the current APS pinhole camera, $\lambda = 100$ pm, $S = 9$ m, and $a_s = 44$ μ m. The measured resolution of 22 μ m is not too far from that shown Figure 1, considering other factors of degradation of the instrument resolution. Further improvement requires shortening the x-ray wavelength or decreasing the source distance S . Employing the first approach requires additional x-ray filters, which would reduce the signal strength; therefore, we decided to take the second approach. By positioning the new pinhole assembly about 3.8 m from the bending magnet source, a decrease in the source distance and an increase on the magnification M together reduce the natural length at the source plane by a factor of two. With commensurate effort in reducing other contributions to the instrument resolution, we expect to improve the total resolution by a factor of two. Furthermore, the increase of the acceptance angle of the pinhole aperture would make it possible for us to use harder x-rays for imaging. Thus, further improvements in resolution can be expected.

3. Mechanical Design

Designing a pinhole system closer to the bending magnet source proved to be quite a challenging task since the only available space is between girders 4 and 5 of (Fig. 2). This space between the flanges is only 43 mm and is crowded by front-end components, various magnets, and water connections.

Additionally, the pinhole system has to meet the following stringent design requirements:

- Ability to survive for up to 300 mA of beam current. This corresponds to a peak power density of 161 W/mm^2 from the dipole radiation.
- Independently movable scrapers with submicron positional accuracy.
- Isolation from the upstream and downstream vacuum chambers in order to suppress the effects of the chambers' vibrations and residual displacements from bakeouts.
- Thermally stable support structure with temperature fluctuations of less than $\pm 0.1 \text{ }^\circ\text{C}$.

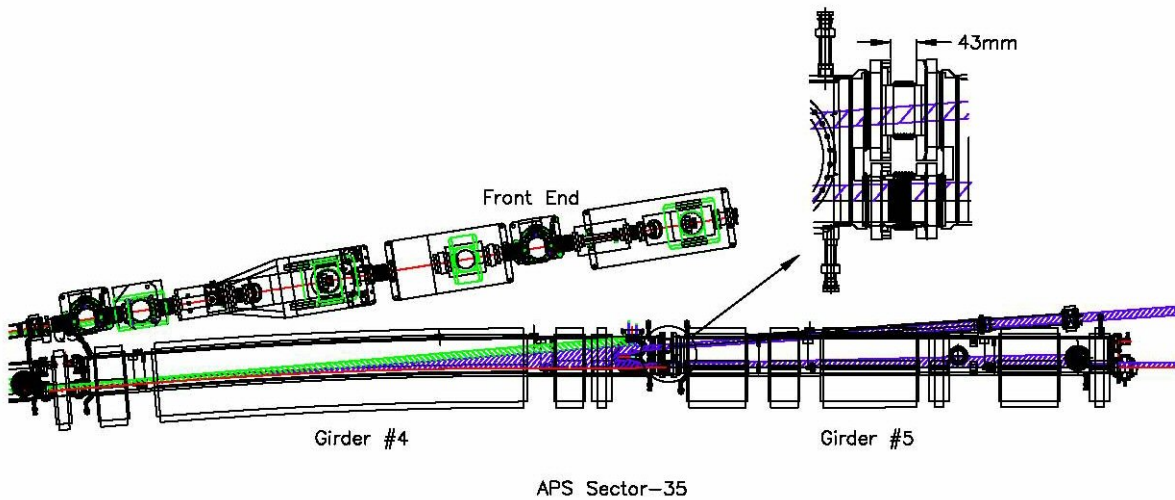


Figure 2: Plan view of girders 4 and 5 of the APS Sector 35.

The main components of the pinhole system are: (1) an upstream pinhole absorber that intercepts most of the dipole radiation, (2) a pinhole bellows assembly to house four scrapers, (3) water-cooled scrapers mounted on precision translation stages, and (4) a thermally stabilized support structure.

3.1. Upstream Pinhole Absorber

Figure 3 shows a plan view of the new upstream absorber assembly consisting of the existing crotch (1) and wedge (2) absorbers, and the pinhole absorber (3). As shown in Fig. 3, the pinhole absorber intercepts an additional sliver of the dipole x-ray fan to shadow the pinhole scrapers located 0.3 m downstream. The normal peak power density of the impinging x-rays is 189 W/mm^2 at 300 mA of beam current. A 0.5-mm round aperture in this absorber allows a narrow beam of only about 30 W to be seen by the scraper rods. The pinhole absorber is attached to a drive mechanism to allow remote-controlled vertical motion of the aperture. This allows placement of the aperture at the center of the x-ray beam profile, accommodating any vertical offset from its nominal position. A 3-D model of the pinhole absorber shadowing downstream scraper rods is shown in Fig. 4.

A design approach used previously for the crotch absorbers was adopted for making the pinhole absorber. The water-to-vacuum braze joint is made first, covering the water channels. A stainless steel (SS-304) cover is then brazed and welded to the bellows shown in Fig. 4. The absorber's body is made from Glidcop® because of its high strength at elevated temperatures. The beam is intercepted by the bottom surface of the absorber at a shallow vertical angle of 11° . Additionally, 1.5-mm-deep fins are machined into this surface to split the impinging beam into two parts: one is intercepted by the top of the fins and the other is intercepted by the bottom of the channels. Based on previous analyses done for the crotch absorbers, a maximum temperature of only $153 \text{ }^\circ\text{C}$ is expected at the top of the fins.

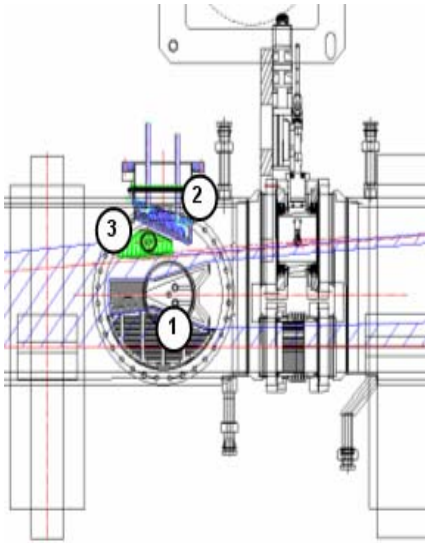


Figure 3: Plan view of upstream absorber assembly.



Figure 4: Pinhole absorber.

3.2. Pinhole Bellows Assembly

A compact bellows assembly, shown in Fig. 5(a), was designed to fit in the available space and house the scraper rods. The main body (4) of this assembly, made from stainless steel (SS-304), is welded to the bellows (5), which are then welded to upstream and downstream rotatable 6-in (152.4-mm) Conflat flanges. This configuration allows the bellows assembly to float between the mating flanges of the chambers on girders 4 and 5 during bakeouts. The floating configuration also allows mounting and alignment of the scrapers rods independent of these two chambers. Four knife-edges (6) are machined directly on the main body (4) to provide a vacuum interface between the body and the scrapers. The nominal width of this assembly is 90 mm, as shown in Fig. 5(b), but the compressed width for installation is only 71 mm.

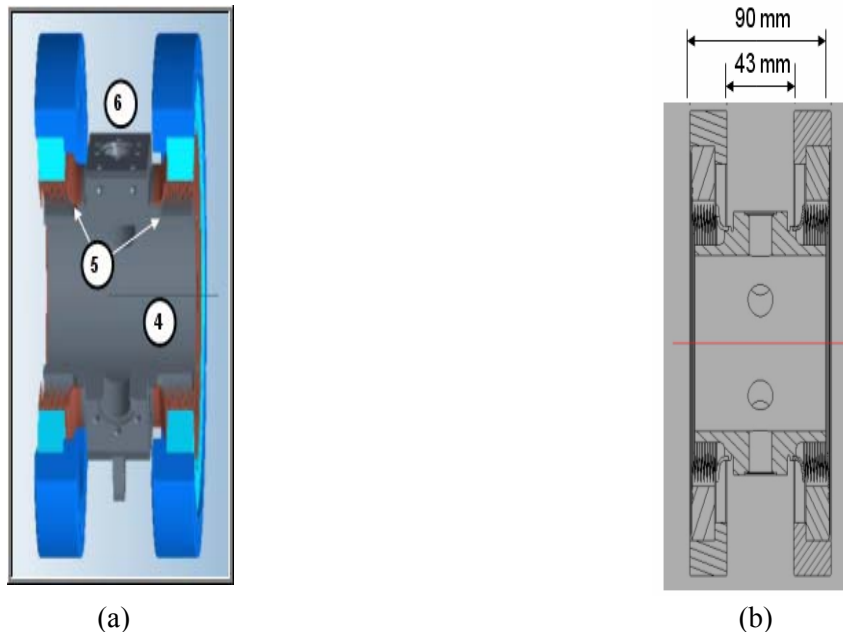


Figure 5: Pinhole bellows assembly, (a) main components, (b) cross section view.

3.3 Water-Cooled Scraper Assemblies

Figure 6 shows four water-cooled scrapers installed on the pinhole bellows assembly. The scraper rods are oriented so that their tungsten tips intercept only the round beam exiting the pinhole absorber while staying clear of the remainder fan of the dipole beam (Fig. 7). These tips (7), shown in the inset of Fig. 7, are given distinct shapes in order to change the size of the pinhole by translation of the scraper rods. The tips are staggered along the beam direction, which allows them to reduce the pinhole size as small as required without the risk of physical interference.

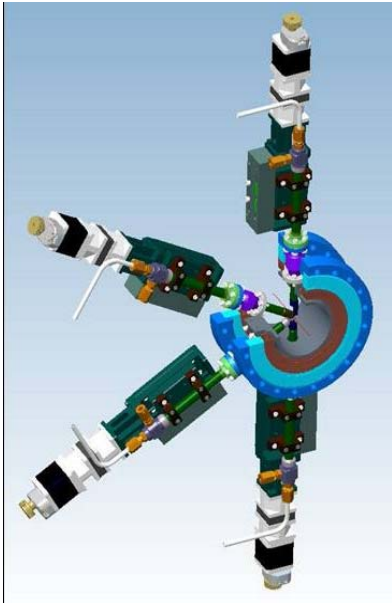


Figure 6: Water-cooled scraper assemblies.

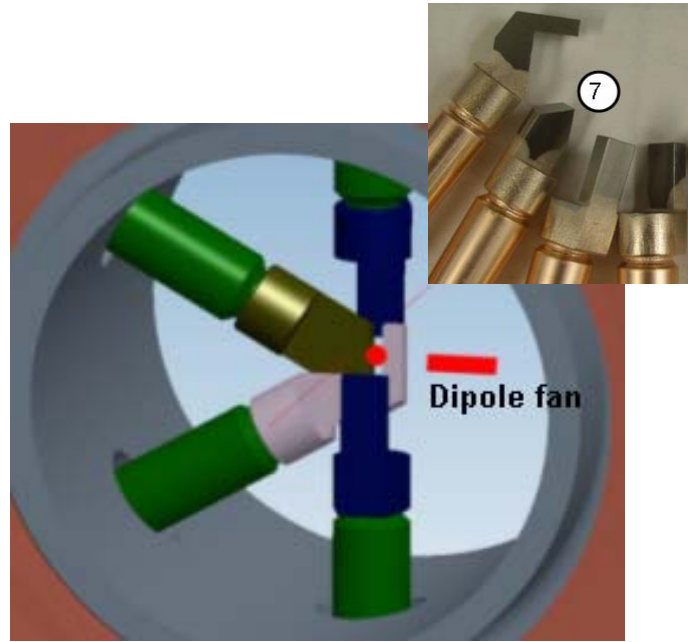


Figure 7: Scraper rods – orientation and tungsten tips.

The tungsten tips are brazed to the Glidcop® rods with 50-50 copper-gold alloy, as shown in Fig. 8. Round 7-mm-diameter bores are pre-drilled into the rods up to 5 mm from the brazing end. These allow counter-flow cooling of the tungsten blades without water-to-vacuum joints. Two SS-304 rings are also brazed to each rod for subsequent welding of a mounting flange (8) and a water manifold (9). A 1-in (25.5-mm) bellows is then welded to this mounting flange and another flange that mates with the machined knife-edge of the pinhole bellows assembly.

Each of the scraper rods is mounted on a Bayside Motion ® precision translation stage (10), as seen in Fig. 9. With a 10:1 gear reducer (11), the table provides a resolution of 0.5 microns for each full step of the Size-17 stepper motor (12). A rotary encoder (13) provides digital feedback on the scraper's motion.

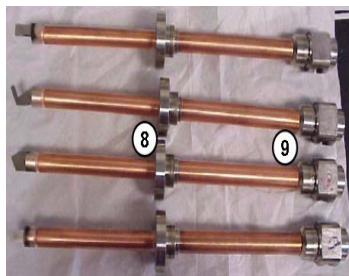


Figure 8: Pinhole scraper rods.

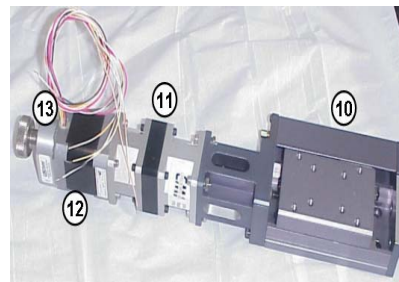


Figure 9: Precision translation stage for scrapers.

3.4 Thermally-Stabilized Support Structure

The translation stages are fastened to a 1-in (25.4-mm)-thick mounting plate (14) made of SS-304 (see Fig. 10). This mounting plate is in turn bolted to a SS-304 support stand grouted to the floor. For structural and vibrational stability, the support stand is made from a 10.75-in (273-mm)-diameter cylinder with a wall thickness of 0.5-in (12.7-mm).

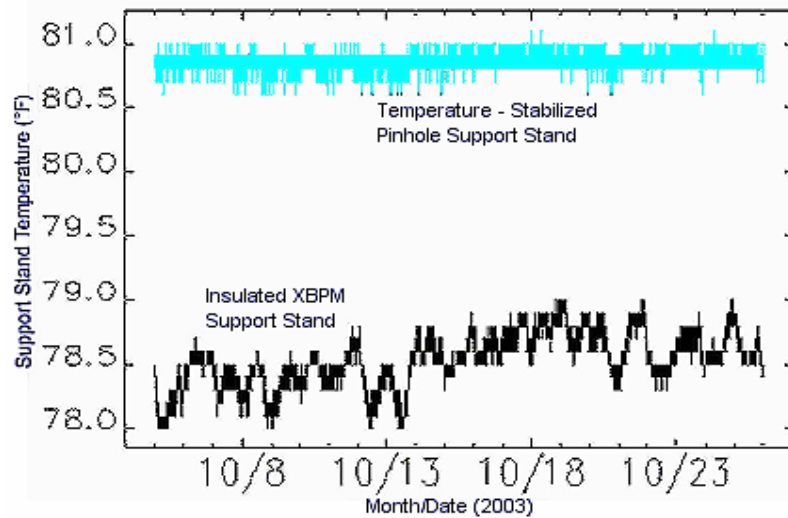
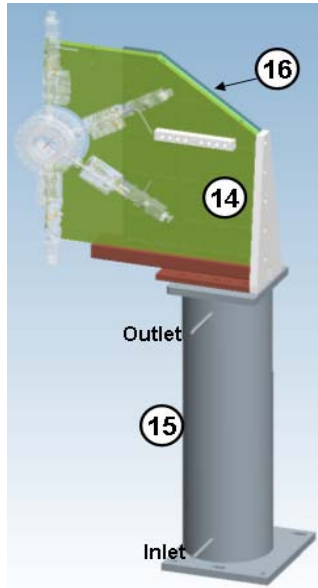


Figure 10: Pinhole support structure. Figure 11: Temperature stability of two types of support stands.

Air temperature in the APS storage ring tunnel has a nominal regulation of ± 1 °C; however, temperature fluctuations have often been as large as ± 3 °C. The resulting vertical displacement of the pinhole at 1.4 m from the floor can, therefore, be as much as ± 50 μm .

Temperature regulation of the APS storage ring water systems was recently improved to ± 0.1 °C [5]. We took advantage of this improvement to thermally stabilize the pinhole support structure. As shown in Fig. 10, the support stand (15) is welded water-tight at its two end with top and bottom 0.5-in (12.7-mm)-thick SS-304 plates. In addition, a water jacket (16) is added to the mounting plate (14). Deionized water enters the support stand from the bottom inlet tube at a low rate of 0.5 GPM (1.9 l/m). It mixes with the large volume of water in the support stand, which dampens its temperature fluctuations. The support stand is thermally insulated on the outside with layers of ceramic cloth in the same manner as the support stand for the x-ray beam position monitors (XBPMs). The mixed water exits from the outlet tube to the cooling jacket of the mounting plate where further mixing takes place with the water contained in the jacket. From there the temperature-stabilized water branches out to the four manifolds of the scraper rods.

Figure 11 compares temperature stability of the pinhole support stand with that of a sand-filled XBPM support stand in Sector 32. The XBPM stand shows temperature fluctuations of about 0.6 °F (0.33 °C) plus a slow drift of the same amount. The pinhole support stand shows temperature fluctuation of only about 0.4 °F (0.17 °C) with essentially no thermal drift.

4. Installation and Initial Testing

Because of highly constrained space between girders 4 and 5 of Sector 35, a detailed assembly, alignment, and installation procedure was developed. A mock-up of this area was created to ensure that the installation could be accomplished as planned. Retaining brackets for the bellows and protective covers for the flanges were used to prevent any damage during installation.

The pinhole absorber was aligned on the bench with respect to the crotch and wedge absorbers. The location of its pinhole aperture was then transferred to an outside (out of the vacuum envelope) fiducial. Similarly, after assembling and aligning the scraper rods on the pinhole bellows assembly, their locations and orientations were transferred to outside fiducials. The scraper rods were then attached with saddle blocks to the translation stages that were snugly bolted to the mounting plate. Linear motion of each rod was verified for its perpendicularity to the beam axis, limit switches were set, and then the translation stages were tightly fastened and pinned to the mounting plate. The scraper rods were then disconnected from both the pinhole bellows assembly and the translation stages for installation in the ring.

The pinhole support stand was installed on the floor and aligned relative to the storage ring magnets. The mounting plate was hoisted with lifting lugs to the top of the support stand and bolted to it. The pinhole bellows assembly was compressed (with brackets designed for this purpose) and inserted between the chamber flanges. The scraper rods were then attached to the pinhole bellows assembly and the translation stages using previously marked fiducials. Finally, the absorber assembly was installed and all water and electrical connections were established.

Initial tests have been done to verify the thermal and mechanical performance of the pinhole components. The scraper rods and their tungsten tips have shown no sign of overheating due to proper shadowing by the pinhole absorber. The scrapers assemblies have performed as expected in terms of changing the pinhole size. Dipole beam exiting the aperture of the pinhole absorber has confirmed its vertical positioning and angular alignment. All components, including stepper motor and rotary encoder, have survived intense radiation scattered from the three absorbers.

The effective resolution of the pinhole will be established after the detector has been upgraded and a beryllium window 20 m from the source, which causes scattering and blurring, has been moved. Further tests are also planned to evaluate hard x-ray transmission through the tungsten tips.

5. Summary and Conclusion

Mechanical design of a new pinhole system for the APS Sector 35 diagnostics beamline has been presented. The main components of this system, namely, a pinhole absorber, a pinhole bellows assembly, water-cooled scraper assemblies, and a thermally stabilized support structure, have been described in detail. Initial tests have confirmed the thermal and mechanical performance of these components.

6. Acknowledgments

The authors thank M. Bracken, W. Jansma, and C. Putnam for valuable assistance during the assembly alignment and testing of this pinhole system. Thanks are also due to C. Eyberger for editing this paper. This work was supported by the U.S. Department of Energy, Office of Basic Energy Sciences, under contract number W-31-109-ENG-38.

7. References

- [1] B.X. Yang, A.H. Lumpkin, "Particle-Beam Profiling Techniques on the APS Storage Ring," 1996 Beam Instrumentation Workshop, Argonne, IL, May 6-9, 1996, A.H. Lumpkin, C.E. Eyberger (Eds.), AIP Conference Proceedings 390, pp. 491-497 (1997).
- [2] B. Yang, A.H. Lumpkin, L. Emery and M. Borland, "Recent Developments in Measurement and Tracking of the APS Storage Ring Beam Emittance," Beam Instrumentation Workshop 2000: Ninth Workshop, Cambridge, MA, May 8-11, 2000, AIP Conference Proceedings 546, pp. 622-633 (2000).
- [3] L. Emery and M. Borland, "Possible Long-Term Improvements to the Advanced Photon Source," Proc. of the 2003 Particle Accelerator Conference, Portland, OR, May 12-16, 2003, pp. 256-258 (2003).
- [4] B. Yang "Optical System Design for High-Energy Particle Beam Diagnostics" Beam Instrumentation Workshop 2002: Tenth Workshop, Upton, NY, May 6-9, 2002, AIP Conference Proceedings 648, pp. 59-78 (2002).
- [5] C. Putnam and R. Dortwegt, "Improved Temperature Regulation of Process Water Systems for the APS Storage Ring," MEDSI 2002, Argonne, IL, September 5-6, 2002, pp. 454-461 (2003).